Domain hierarchy in annealed (001)-oriented Pb (Mg 1 3 Nb 2 3) O 3 - x % PbTiO 3 single crystals

Feiming Bai, JieFang Li, and D. Viehland

Citation: Applied Physics Letters **85**, 2313 (2004); doi: 10.1063/1.1793353
View online: http://dx.doi.org/10.1063/1.1793353
View Table of Contents: http://scitation.aip.org/content/aip/journal/apl/85/12?ver=pdfcov
Published by the AIP Publishing

Domain hierarchy in annealed (001)-oriented $Pb(Mg_{1/3}Nb_{2/3})O_3$-x%$PbTiO_3$ single crystals

Feiming Bai, JieFang Li, and D. Viehland[a)]
Department of Materials Science and Engineering, Virginia Tech, Blacksburg, Virginia 24061

(Received 28 April 2004; accepted 26 July 2004)

The domain structures of annealed (001)-oriented $Pb(Mg_{1/3}Nb_{2/3})O_3$-x%$PbTiO_3$(PMN-x%PT) crystals for $x=10$, 20, 30, 35, and 40 at.% have been investigated by polarized optical microscopy and scanning force microscopy in the piezoresponse mode. The results demonstrate the presence of a domain hierarchy on various length scales ranging from 40 nm to 0.1 mm, which varies with x.
 [DOI: 10.1063/1.1793353]

The crystalline solution $Pb(Mg_{1/3}Nb_{2/3})O_3$-x%$PbTiO_3$, PMN-xPT, is known to have complex structure-property relationships. In the unpoled condition for $x\approx0.35$, a relaxor ferroelectric state is known to exist, characterized by a frequency dispersive dielectric maximum.[1,2] Phase transformation investigations by x-ray diffraction (XRD) and neutron scattering have shown a tetragonal T phase for $x>0.35$, a monoclinic M_c phase for $30<x<35$, a rhombohedral R phase for $0.25\approx x<0.30$,[3,4] and a slightly distorted pseudocubic phase designated as X for $x<0.25$.[5,6] Corresponding to these structural studies, counterpart investigations of the domain structure evolution with increase of PT content have also been performed by polarized optical microscopy (POM),[7–9] and transmission electron microscopy (TEM).[10–12] However, due to limited resolution, optical microscopy does not reveal details of domain configurations, but rather only provides a representative domain structure averaged throughout the specimen thickness. Also, by TEM, the high energy of electron beams can alter the domain distribution,[12] making it difficult to identify whether hierarchal domain structures exist on various length scales.

Recent developments in scanning force microscopy (SFM), performed in the piezoresponse mode (or PFM), offer an alternative way to observe the domain structure of ferroelectric materials.[13,14] This technique is based on the detection of local vibrations of a ferroelectric sample induced by a testing ac signal applied between the conductive tip of the SFM and the bottom electrode of the sample. The oscillations of the sample underneath the tip modulate the global deflection signal and are detected using a lock-in technique.[14] Recently, investigations of PZN-8%PT and PMN-29%PT single crystals have been performed using PFM.[15] Small irregular domain structures were observed in the poled condition in both vertical and lateral piezoelectric modes, whereas large antiparallel domains were found in the unpoled condition. The dependence of the domain structure on orientation has also been reported for unpoled PZN-4.5%PT crystals.[16] In the unpoled condition, small irregular domains were reported on (001)-oriented surfaces; whereas for (111) cuts, normal micron-sized domains oriented along permissible crystallographic planes were found.

The purpose of this investigation was to study the evolution of the domain structure with composition for (001)-oriented PMN-xPT crystals by piezoresponse force microscopy. Investigations have focused on revealing how the domain structure changes between phases X, R, M_c, and T with increasing x from a zero-field-cooled (ZFC) condition. Our results demonstrate the presence of a domain hierarchy on various lengths scales, which varies with x.

Single crystals of (001)-oriented PMN-x%PT ($x=10$, 20, 30, 35, and 40) were grown by a top-seeded modified Bridgman method.[17,18] The crystals were cut into plates with typical dimensions of $4\times4\times0.3$ mm^3. The top faces of the crystals were polished to 0.25 μm finishes. Before measurements were begun, all crystals were annealed at 550 K for 30 min to remove surface stresses. Careful investigations were performed by POM, starting from the annealed condition. Gold electrodes were deposited on the bottom face of each sample by sputtering. The electroded face was then glued to the SFM sample stage, and the opposite unelectroded surface was subjected to SFM tip scanning. SFM images were obtained in the piezoresponse mode using commercial equipment (DI 3100a by Vecoo). All scans were

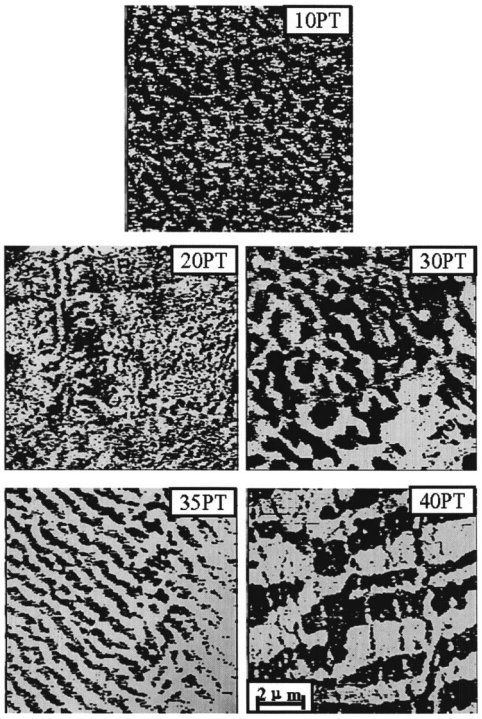

FIG. 1. Piezoresponse force images for various (001)-oriented PMN-x%PT crystals.

[a)]Electronic mail: viehland@mse.vt.edu

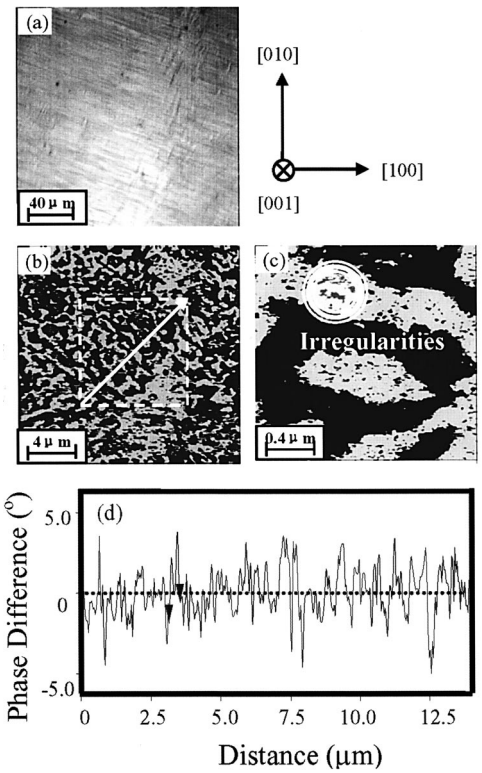

FIG. 2. Domain hierarchy of (001)-orientated PMN-30%PT in *R* phase. (a) Spindle-like macrodomain plates with a ⟨110⟩ type preferred orientation by POM; (b) wave-like self-assembled domains by PFM; (c) high-resolution PFM image illustrating nonsmooth domain boundaries and irregularity; and (d) cross-sectional line analysis normal to [110].

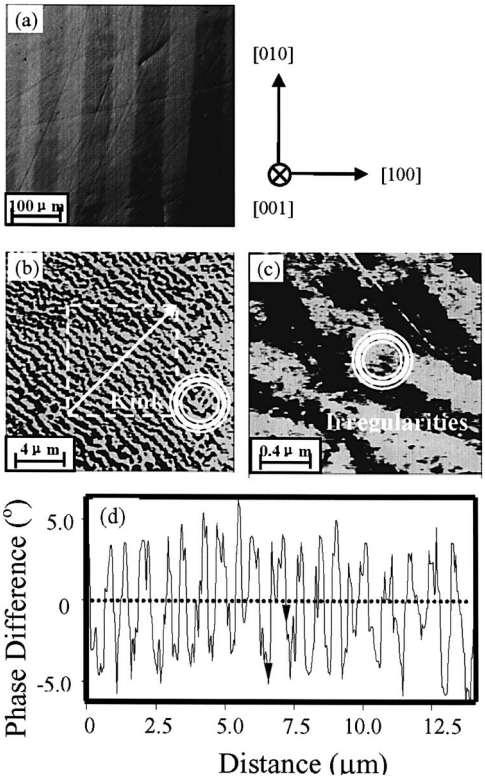

FIG. 3. Domain hierarchy of (001)-orientated PMN-35%PT in M_c phase. (a) Stripe-like macrodomain plates with a [010]-type preferred orientation by POM; (b) microdomain striations with a ⟨110⟩ type preferred orientation by PFM, (kinks are illustrated at boundaries); (c) high-resolution PFM image, illustrating nonsmooth domain boundaries and irregularities; and (d) cross-sectional line analysis normal to [110].

performed at room temperature, using a conductive silicon tip coated with cobalt. An ac voltage with a frequency of 20 kHz and amplitude from 1 and 10 V was applied between the conductive tip and the bottom gold electrode.

Figure 1 shows PFM images of unpoled (001)-oriented PMN-*x*PT crystals for various *x* values between 10 and 40 at.%. Polar nanodomains were observed in PMN-10%PT, which had an irregular morphology and distribution. The size of these domains was about 40 nm, which is very close to the tip resolution limit (20 nm). With increasing PT content to 20 at.%, the size of the PNDs was not changed, but their density increased and they began to form into regular patterns. However, presumably due to compositional fluctuations, the degree of regularity varied somewhat from area to area. For 30%PT, the size of PNDs was notably increased, and their distribution became much more regular. This resulted in the gradual development of an anisotropic domain morphology, with preferential alignment close to a ⟨110⟩ type direction. With increasing *x* to 35 at.%, a self-assembly of PND into long and thin domain striations, oriented close to a ⟨110⟩, became apparent. The domain lengths were on the order of tens of microns, whereas the widths were much less. For PMN-40%PT, microsized tetragonal domains were observed with a preferred ⟨001⟩ type orientation. The domain lengths were on the order of tens of microns, and the widths were on the order of several microns.

For (001)-oriented PMN-10%PT, which is of the *X* phase,[4–6] POM revealed a featureless image. However, the corresponding PFM image, shown above, revealed the presence of PND. Comparison of these results show that phase *X* consists of PND, which do not self-assemble into macrodomain plates. The PND are essentially nonstress accommodating, and thus their boundaries are not restricted by elastic compatibility. A similar domain structure was observed for PMN-20%PT. However, with increasing PT concentration, more regular domain patterns became evident, as to be shown below, indicating an importance of stress accommodation.

Figure 2 shows POM and PFM images taken over various lengths scales for (001)-orientated PMN-30%PT, which is of the *R* phase.[3,4] Figure 2(a) shows a POM image that reveals rhombohedral macrodomain plates twined close to a ⟨110⟩, which have a spindle-like morphology. The macrodomain widths are $\sim 1\ \mu$m and their lengths are $\sim 20\ \mu$m. Inside the macrodomain plates, miniature "wavy" domains oriented close to a ⟨110⟩ were found, as shown in the PFM image of Fig. 2(b). A higher-resolution PFM image, shown in Fig. 2(c), illustrates that the domain boundaries are rough, and that there are irregularities of similar size to PND internal to the "wavy" domains. In Fig. 2(d), cross-sectional line analysis along the [110] direction revealed an average domain spacing of $\sim 0.34\ \mu$m, where the phase difference fluctuated pronouncedly as a function of distance.

Figure 3 shows the domain hierarchy for (001)-orientated PMN-35%PT, which is of the M_c phase.[3,4] Broad stripe-like domains oriented close to a ⟨001⟩ direction were found by POM, as shown in Fig. 3(a). The average domain width was $\sim 50\ \mu$m. Inside the macrodomain plates, alternating domain striations oriented close to a ⟨110⟩ were found that had a width of $<0.5\ \mu$m, as shown in the PFM image of Fig. 3(b). Kinks between neighboring striations, illustrated

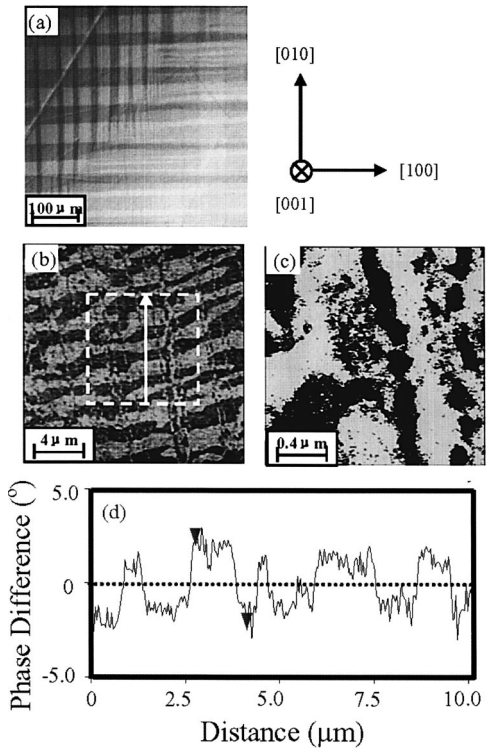

FIG. 4. Domain hierarchy of (001)-orientated PMN-40%PT in *T* phase. (a) Stripe-like macrodomain plates with a ⟨100⟩ type preferred orientation by POM; (b) ⟨100⟩ orientated stripe-like microdomains with fibrous subdomain structures by PFM; (c) high-resolution PFM image, illustrating domain irregularity; and (d) cross-sectional line analysis normal to [100].

by a circle, are 90° twins between them. A higher-resolution PFM image is given in Fig. 3(c). The striations can be seen to be rough and nonuniform in thickness, having internal irregularities of similar size to PND. Cross-sectional line analysis, shown in Fig. 3(d), yielded an average domain spacing of $\sim 0.35\ \mu$m. In addition, the analysis indicated pronounced contrast variation within a domain, as illustrated by the peaks between two triangles, which may be subdomain structures corresponding to PNDs in Fig. 3(c).

The domain hierarchy of PMN-40%PT is shown in Fig. 4, which is of the *T* phase.[3,4] Stripe-like tetragonal domains oriented close to a ⟨001⟩ are apparent in the POM image of Fig. 4(a). These macrodomain plates are similar to those of PMN-35%PT, except for thin 90° fringes, indicative of a larger transformation stress. Internal to the macrodomains, fine broken domain striations were found that were oriented close to a ⟨001⟩, as can be seen in the PFM image of Fig. 4(b). Their lengths varied from several to $\sim 30\ \mu$m. It is relevant to note that these macrodomains and internal striations were both oriented along the same direction, unlike that for PMN-35%PT. Fig. 4(c) shows a higher-resolution PFM image, revealing that the striations are quite rough. Cross-sectional analysis taken along the [010], shown in Fig. 4(d), reveals an average domain spacing of $\sim 2\ \mu$m that fluctuated notably, possibly reflecting the domain heterogeneities in Fig. 4(c).

In summary, our results demonstrate a domain hierarchy on various length scales between nano- and milli-meters. Observations can be summarized with respect to relevant phases. Phase *X* consists of PND, which do not self-assemble into macrodomain plates. Phase $R(x=30\%)$ consists of PND that begin to self-assemble into colonies close to a ⟨110⟩, which is spatially limited to $<1\ \mu$m. Colonies then assemble into macrodomain plates oriented close to ⟨111⟩. Phase $Mc(x=35\%)$ consists of miniature polar domains, which self-assemble into ⟨110⟩ striations of a scale $<1\ \mu$m. Alternating striations then assemble into macrodomain plates of mm size, which are oriented close to a ⟨001⟩. Whereas, phase $T(x=40\%)$ consists of ⟨001⟩ oriented striations of μm size that have an internal nanoscale heterogeneity, which self-assemble into macrodomain plates of mm size oriented along a ⟨001⟩.

The authors gratefully acknowledge the support of the Office of Naval Research under Grant Nos. N000140210340, N000140210126, and MURI N000140110761.

[1]G. A. Smolenskii and A. Agranovskaya, Sov. Phys. Solid State **1**, 1429 (1960).
[2]L. E. Cross, Ferroelectrics **151**, 305 (1994).
[3]B. Noheda, D. E. Cox, Shirane, J. Gao, and Z. Ye, Phys. Rev. B **66**, 054104 (2002).
[4]J. M. Kiat, Y. Uesu, B. Dkhil, M. Matsuda, C. Malibert, and G. Calvarin, Phys. Rev. B **65**, 064106 (2002).
[5]G. Xu, D. Viehland, J. F. Li, P. M. Gehring, and G. Shirane, cond-mat/0307144.
[6]P. M. Gehring, W. Chen, Z.-G. Ye, and G. Shirane, cond-mat/0304289.
[7]C.-S. Tu, C.–L. Tsai, V. H. Schimidt, H. Luo, and Z. Yin, J. Appl. Phys. **89**, 7908 (2001).
[8]G. Xu, H. Luo, H. Xu, and Z. Yin, Phys. Rev. B **64**, 020102 (2001).
[9]C. Tu, I. Shih, V. Schmidt, and R. Chien, Appl. Phys. Lett. **83**, 1833 (2003).
[10]C. Randall, D. Barber, and R. Whatmore, J. Microsc. **45**, 275 (1987).
[11]D. Viehland, M.-C. Kim, Z. Xu, and J.-F. Li, Appl. Phys. Lett. **67**, 2471 (1995).
[12]Z. Xu, M.-C. Kim, J.-F. Li, and D. Viehland, Philos. Mag. A **74**, 395 (1996).
[13]M. Abplanalp, L. M. Eng, and P. Gunter, Appl. Phys. A: Mater. Sci. Process. **66**, S231 (1998).
[14]C. Harnagea, Ph. D. Dissertation, Martin-Luther University, Halle-Wittenberg, Germany, 2001.
[15]M. Abplanalp, D. Barosova, J. Erhart, J. Fousek, P. Gunter, J. Nosek, and M. Sulc, J. Appl. Phys. **91**, 3797 (2002).
[16]K. Bdikin, V. V. Shvartsman, and A. L. Kholkin, Appl. Phys. Lett. **83**, 4232 (2003).
[17]W. Tan, Z. Xu, J. Shang, and P. Han, Appl. Phys. Lett. **76**, 3732 (2000).
[18]W. Zhu and P. Han, Appl. Phys. Lett. **75**, 3868 (1999).